Journal of Computational Physics 348 (2017) 776–789

Contents lists available at ScienceDirect

Journal of Computational Physics

www.elsevier.com/locate/jcp

Unconditionally stable Gauge–Uzawa finite element schemes for incompressible natural convection problems with variable density ☆

Jilian Wu [a], Jie Shen [b,*], Xinlong Feng [a]

[a] College of Mathematics and Systems Science, Xinjiang University, Urumqi 830046, PR China
[b] Department of Mathematics, Purdue University, West Lafayette, IN 47907, USA

ARTICLE INFO

Article history:
Received 9 May 2017
Received in revised form 21 July 2017
Accepted 24 July 2017
Available online 4 August 2017

Keywords:
Natural convection
Variable density
Gauge–Uzawa
Finite element method
Stability analysis

ABSTRACT

We construct in this paper two Gauge–Uzawa schemes, one in conserved form and the other in convective form, for solving natural convection problems with variable density, and prove that the first-order versions of both schemes are unconditionally stable. We also show that a full discretized version of the conserved scheme with finite elements is also unconditionally stable. These schemes lead to a sequence of decoupled elliptic equations to solve at each step, hence, they are very efficient and easy to implement. We present several numerical tests to validate the analysis and demonstrate the effectiveness of these schemes for simulating natural convection problems with large density differences.

1. Introduction

We consider in this paper numerical approximations of natural convection (NC) equations of an incompressible viscous Newtonian fluid with variable density [20]:

$$\begin{cases} \rho_t + (\mathbf{u}\cdot\nabla)\rho = 0 & \text{in } \Omega\times(0,T_1] \quad \text{(a)},\\ \rho(\mathbf{u}_t + (\mathbf{u}\cdot\nabla)\mathbf{u}) - \mu\Delta\mathbf{u} + \nabla p = \rho\mathbf{g} & \text{in } \Omega\times(0,T_1] \quad \text{(b)},\\ \nabla\cdot\mathbf{u} = 0 & \text{in } \Omega\times(0,T_1] \quad \text{(c)},\\ \rho(T_t + (\mathbf{u}\cdot\nabla)T) - \kappa\Delta T = 0 & \text{in } \Omega\times(0,T_1] \quad \text{(d)}, \end{cases} \tag{1.1}$$

where the unknown functions are the density $\rho > 0$, the velocity vector $\mathbf{u}$, the pressure p and the temperature T; μ, κ, $T_1 > 0$ and $\mathbf{g}$ represent the dynamic viscosity coefficient, the thermal conductivity parameter, the fixed time and the gravitational force, respectively; Ω is an open bounded domain in $\mathbb{R}^d$ ($d = 2$ or 3) with a sufficiently smooth boundary $\partial\Omega$. The above system is derived, under the assumptions that the energy depends only on the temperature and that the specific heat at constant volume is a constant, from the mass conservation, momentum conservation, incompressibility and the energy conservation. More details can be found in [1,4,20].

☆ The work of J. Shen is supported in part by NSF DMS-1620262 and AFOSR FA9550-16-1-0102. The work of X. Feng is supported in part by the NSF of China grant No. 11362021, 11671345, and NSF of Xinjiang Province No. 2016D01C058.

* Corresponding author.
E-mail addresses: math_wjl@163.com (J. Wu), shen@math.purdue.edu (J. Shen), fxlmath@gmail.com (X. Feng).

http://dx.doi.org/10.1016/j.jcp.2017.07.045
0021-9991/

The system (1.1) is supplemented with the following initial and boundary conditions for ρ, $\mathbf{u}$ and T:

$$\begin{cases} \mathbf{u}(\mathbf{x},0)=\mathbf{u}_0(\mathbf{x}) \quad \text{in } \Omega \quad \text{and} \quad \mathbf{u}(\mathbf{x},t)|_{\Gamma}=\mathbf{g}_1(\mathbf{x},t), \\ \rho(\mathbf{x},0)=\rho_0(\mathbf{x}) \quad \text{in } \Omega \quad \text{and} \quad \rho(\mathbf{x},t)|_{\Gamma_{\mathbf{u}(\mathbf{x},t)}}=r(\mathbf{x},t), \\ T(\mathbf{x},0)=T_0(\mathbf{x}) \quad \text{in } \Omega \quad \text{and} \quad \dfrac{\partial T(\mathbf{x},t)}{\partial \mathbf{n}}\Big|_{\Gamma_1}=0, \quad T(\mathbf{x},t)|_{\Gamma_2}=g_2(\mathbf{x},t), \end{cases} \tag{1.2}$$

where $\Gamma=\partial\Omega$, Γ_1 is a regular open subset of Ω, $\Gamma_2=\partial\Omega\setminus\Gamma_1$, and for any velocity field $\mathbf{v}$, $\Gamma_{\mathbf{v}}$ is the inflow boundary defined by $\Gamma_{\mathbf{v}}=\{\mathbf{x}\in\Gamma:\mathbf{v}(\mathbf{x})\cdot\mathbf{n}<0\}$ with $\mathbf{n}$ being the outward unit normal vector. Throughout this paper we assume that the boundary Γ is impermeable, i.e., $\mathbf{u}\cdot\mathbf{n}=0$ everywhere on Γ and $\Gamma_{\mathbf{v}}=\emptyset$. We note that no initial and boundary condition is needed for the pressure p which can be viewed as a Lagrange multiplier whose mathematical role is to enforce the incompressibility condition.

NC phenomena are found in many scientific and engineering applications, and have been intensively studied in the literature, cf. [2,20,22,24,25]. When the density variation is small, it can be modeled by using a Boussinesq approximation [20], which treats the density as a constant but with an added buoyancy force as follows:

$$\begin{cases} \mathbf{u}_t-\nu\Delta\mathbf{u}+(\mathbf{u}\cdot\nabla)\mathbf{u}+\nabla p=Ra\mathbf{j}T & \text{in } \Omega\times(0,T_1], \\ \nabla\cdot\mathbf{u}=0 & \text{in } \Omega\times(0,T_1], \\ T_t-\kappa\Delta T+(\mathbf{u}\cdot\nabla)T=\gamma & \text{in } \Omega\times(0,T_1], \end{cases} \tag{1.3}$$

where $\nu=\frac{1}{Re}$, $\kappa=\frac{\nu}{Pr}$, Ra, Pr, Re is the Rayleigh number, the Prandtl number, and the Reynolds number, respectively. Most of the studies on the NC phenomena are based on the Boussinesq approximation [5,11,18,19,21–24,26].

However, in most geophysical flows, the temperature difference is the driving mechanism of the fluid motion. They are often driven by large temperature differences which lead to considerable density variations under which the Boussinesq approximation is no longer valid. In these cases, we are led to consider the model (1.1).

Constructing stable and efficient numerical schemes for the system (1.1)–(1.2) is challenging since it involves all the difficulties associated with the density-dependent Navier–Stokes equations as well as additional difficulties introduced by the temperature equation. Some numerical difficulties are: (i) the coupling of the velocity and pressure through the incompressibility constraint, (ii) the presence of nonlinear terms, (iii) the coupling of flow field and temperature field, (iv) the transport equation for the density is of hyperbolic type while the others are of parabolic type. The objective for this paper is to design efficient and unconditionally energy stable numerical schemes to solve the coupled system (1.1)–(1.2).

For the incompressible Navier–Stokes equations with variable density, several stable schemes based on projection methods have been constructed in [9,12,16]. The schemes in [16] are based on the Gauge–Uzawa formulation [13–15] which has some advantages over the original Gauge method [7] and the pressure-correction projection method [17] for incompressible flows: (i) it does not require an artificial boundary condition on pressure, (ii) it does not require an initial pressure, (iii) its convergence is proved under minimal smoothness assumptions [10]. Hence, we shall extend the Gauge–Uzawa schemes in [16] for Navier–Stokes equations with variable density to the NC equations with variable density (1.1).

The system (1.1) is written in convective form which is not very convenient for analysis. We can rewrite (1.1) in a conservative form which is better suited for deriving energy dissipation laws. Following [8,16], we introduce $\sigma=\sqrt{\rho}$ and derive from (1.1a) and (1.1c) that

$$\begin{cases} \sigma(\sigma\mathbf{u})_t=\rho\mathbf{u}_t+\dfrac{1}{2}\rho_t\mathbf{u}=\rho\mathbf{u}_t-\dfrac{\mathbf{u}}{2}(\mathbf{u}\cdot\nabla\rho), \\ \sigma(\sigma T)_t=\rho T_t+\dfrac{1}{2}\rho_t T=\rho T_t-\dfrac{T}{2}(T\cdot\nabla\rho). \end{cases}$$

Using the above identities, we can rewrite (1.1) as:

$$\begin{cases} \rho_t+(\mathbf{u}\cdot\nabla)\rho+\dfrac{\rho}{2}\nabla\cdot\mathbf{u}=0, & \text{in } \Omega\times(0,T_1] \quad \text{(a)}, \\ \sigma(\sigma\mathbf{u})_t+(\rho\mathbf{u}\cdot\nabla)\mathbf{u}+\dfrac{\mathbf{u}}{2}(\mathbf{u}\cdot\nabla\rho)-\mu\Delta\mathbf{u}+\nabla p=\rho\mathbf{g} & \text{in } \Omega\times(0,T_1] \quad \text{(b)}, \\ \nabla\cdot\mathbf{u}=0 & \text{in } \Omega\times(0,T_1] \quad \text{(c)}, \\ \sigma(\sigma T)_t+(\rho\mathbf{u}\cdot\nabla)T+\dfrac{T}{2}(\mathbf{u}\cdot\nabla\rho)-\kappa\Delta T=0 & \text{in } \Omega\times(0,T_1] \quad \text{(d)}. \end{cases} \tag{1.4}$$

Note that the term $\frac{\rho}{2}\nabla\cdot\mathbf{u}=0$ in Ω because of the incompressibility condition (1.1c). A main advantage of the above formulation is that the nonlinear terms of (1.4) satisfy the following desired properties: for ρ, $\mathbf{u}$, $\mathbf{v}$, T smooth enough and $\mathbf{u}\cdot\mathbf{n}|_{\Gamma}=0$, we have

$$\begin{cases} \int_\Omega (\mathbf{u}\cdot\nabla\rho)\rho d\mathbf{x} = 0 \text{ and } \frac{1}{2}\int_\Omega \rho\nabla\cdot\mathbf{u}\rho d\mathbf{x} = 0 \quad \text{(a)}, \\ \int_\Omega (\rho\mathbf{u}\cdot\nabla\mathbf{v})\cdot\mathbf{v} d\mathbf{x} + \frac{1}{2}\int_\Omega (\mathbf{u}\cdot\nabla\rho)\mathbf{v}\cdot\mathbf{v} d\mathbf{x} = 0 \quad \text{(b)}, \\ \int_\Omega (\rho\mathbf{u}\cdot\nabla T)T d\mathbf{x} + \frac{1}{2}\int_\Omega (\mathbf{u}\cdot\nabla\rho)TT d\mathbf{x} = 0 \quad \text{(c)}. \end{cases} \tag{1.5}$$

Hence, taking the inner product of (1.4a), (1.4b) and (1.4d) with $\rho(\mathbf{x},t)$, $\mathbf{u}(\mathbf{x},t)$ and $T(\mathbf{x},t)$, respectively, we obtain the following energy dissipation laws:

$$\begin{cases} \frac{1}{2}\frac{d}{dt}\|\rho(\cdot,t)\|_{L^2}^2 = 0, \\ \frac{1}{2}\frac{d}{dt}\|\sigma(t)\mathbf{u}(\cdot,t)\|_{L^2}^2 + \mu\|\nabla\mathbf{u}(\cdot,t)\|_{L^2}^2 = \int_\Omega \rho(\mathbf{x},t)\mathbf{g}\cdot\mathbf{u}(\mathbf{x},t)d\mathbf{x}, \\ \frac{1}{2}\frac{d}{dt}\|\sigma(t)T(\cdot,t)\|_{L^2}^2 + \kappa\|\nabla T(\cdot,t)\|_{L^2}^2 = 0. \end{cases} \tag{1.6}$$

We shall construct two new Gauge–Uzawa schemes in this paper one for the conserved form (1.4) and the other for the convective form (1.1). The scheme in conserved form is convenient for the analysis but slightly more expensive than the scheme in convective form because of the three additional nonlinear terms in (1.4a), (1.4b) and (1.4d). Generally, the conserved form is more suitable for a Galerkin type spatial discretization while the convective form is more convenient for a collocation type method or finite difference method.

We now introduce some functional spaces to be used in the analysis. We denote the standard scalar Sobolev space by $H^m(\Omega) = W^{m,2}(\Omega)$ $(m = 0, 1, 2, \cdots)$ with norm $\|v\|_m = (\sum_{|\gamma|\le m} \|D^\gamma v\|_0^2)^{1/2}$ where $\|v\|_0^2 = \int_\Omega v^2 dx$. For vector-value functions, we use the Sobolev space $\mathbf{H}^m(\Omega) = (H^m(\Omega))^d$ with norm $|\mathbf{v}|_m = (\sum_{i=1}^d \|v_i\|_m^2)^{1/2}$, where $d = 2$ or 3 is the space dimension and $\mathbf{H}_0^1(\Omega) = \{\mathbf{v}\in\mathbf{H}^1(\Omega) : \mathbf{v}|_{\partial\Omega} = 0\}$. We set $\mathbf{L}^2(\Omega) := (L^2(\Omega))^d$ and denote $L_0^2(\Omega) = \{v\in L^2(\Omega) : \int_\Omega v dx = 0\}$. We use $\langle\cdot,\cdot\rangle$ to denote the inner product in $L^2(\Omega)$ and use C to denote a generic positive constant which may depend on Ω, μ, κ, ρ^0, $\mathbf{u}^0$, T^0, $\mathbf{g}$ and T_1.

The remainder of this paper is organized as follows. In Sections 2–3, we present two first-order semi-discretized and full-discretized Gauge–Uzawa schemes, and prove that they are unconditionally stable, respectively. In addition, we give their corresponding second-order schemes. In Section 4, we firstly give some numerical results which reveal the convergence rate of our schemes for all unknown functions, then we present the simulation of Bénard convection problem to show the efficiency and validness of these schemes. Because of its simplicity and the richness of the phenomena, Bénard problem has been extensively studied both theoretically and experimentally [3,6], and serves as an excellent benchmark problem for numerical schemes. Finally, conclusions are drawn in Section 5.

2. Gauge–Uzawa method in conserved form

In this section, we construct the time discretization schemes for (1.4).

Let $\tau > 0$ be a time step and set $t_n = n\tau$ for $0 \le n \le N = \lfloor T_1/\tau \rfloor$, where $\lfloor\cdot\rfloor$ is the floor function. The time-discrete approximations to $(\rho(t_n), \mathbf{u}(t_n), p(t_n), T(t_n))$ will be denoted by $(\rho^n, \mathbf{u}^n, p^n, T^n)$.

2.1. First-order Gauge–Uzawa scheme

The first-order semi-discrete Gauge–Uzawa method is as follows:

Algorithm 2.1 *(Gauge–Uzawa method in conserved form).* Given $\rho^0 = \rho_0$, $\mathbf{u}^0 = \mathbf{u}_0$, $T^0 = T_0$, and $s^0 = 0$, then repeat the following steps for $1 \le n \le N$:

Step 1. Find ρ^{n+1} as the solution of

$$\begin{cases} \frac{\rho^{n+1}-\rho^n}{\tau} + \mathbf{u}^n\cdot\nabla\rho^{n+1} + \frac{\rho^{n+1}}{2}\nabla\cdot\mathbf{u}^n = 0, \\ \rho^{n+1}|_{\Gamma_{\mathbf{u}^n}} = r^{n+1}. \end{cases} \tag{2.1}$$

Step 2. Find $\tilde{\mathbf{u}}^{n+1}$ as the solution of

$$\begin{cases} \sigma^{n+1}\dfrac{\sigma^{n+1}\tilde{\mathbf{u}}^{n+1}-\sigma^n\mathbf{u}^n}{\tau}+\rho^{n+1}(\mathbf{u}^n\cdot\nabla)\tilde{\mathbf{u}}^{n+1}+\dfrac{\tilde{\mathbf{u}}^{n+1}}{2}(\mathbf{u}^n\cdot\nabla\rho^{n+1})+\mu\nabla s^n-\mu\Delta\tilde{\mathbf{u}}^{n+1}=\rho^{n+1}\mathbf{g}, \\ \tilde{\mathbf{u}}^{n+1}|_\Gamma=\mathbf{g}_1^{n+1}. \end{cases} \tag{2.2}$$

Step 3. Find ϕ^{n+1} as the solution of

$$\begin{cases} -\nabla\cdot(\dfrac{1}{\rho^{n+1}}\nabla\phi^{n+1})=\nabla\cdot\tilde{\mathbf{u}}^{n+1}, \\ \partial_{\mathbf{n}}\phi^{n+1}|_\Gamma=0. \end{cases} \tag{2.3}$$

Step 4. Update $\mathbf{u}^{n+1}$ and s^{n+1} by

$$\begin{cases} \mathbf{u}^{n+1}=\tilde{\mathbf{u}}^{n+1}+\dfrac{1}{\rho^{n+1}}\nabla\phi^{n+1}, \\ s^{n+1}=s^n-\nabla\cdot\tilde{\mathbf{u}}^{n+1}. \end{cases} \tag{2.4}$$

Step 5. Find T^{n+1} as the solution of

$$\begin{cases} \sigma^{n+1}\dfrac{\sigma^{n+1}T^{n+1}-\sigma^nT^n}{\tau}+\rho^{n+1}(\mathbf{u}^{n+1}\cdot\nabla)T^{n+1}+\dfrac{T^{n+1}}{2}(\mathbf{u}^{n+1}\cdot\nabla\rho^{n+1})-\kappa\Delta T^{n+1}=0, \\ T^{n+1}|_\Gamma=g_2^{n+1}. \end{cases} \tag{2.5}$$

Remark 2.1. In practice, (2.3) is often reformulated in the following weak formulation

$$\left\langle\frac{1}{\rho^{n+1}}\nabla\phi^{n+1},\nabla q\right\rangle=-\langle\tilde{\mathbf{u}}^{n+1},\nabla q\rangle,\quad\forall q\in H^1(\Omega). \tag{2.6}$$

We derive from (2.4) and (2.6) that

$$\langle\mathbf{u}^{n+1},\nabla q\rangle=0,\quad\forall q\in H^1(\Omega), \tag{2.7}$$

which implies that in the space continuous case, we have

$$\nabla\cdot\mathbf{u}^{n+1}=0\quad\text{and}\quad\mathbf{u}^{n+1}\cdot\mathbf{n}|_\Gamma=\mathbf{g}_1^{n+1}\cdot\mathbf{n}|_\Gamma. \tag{2.8}$$

However, in the space discrete case, only a discrete version of (2.7) will be satisfied so the discrete velocity field will generally not be divergence free.

Remark 2.2. Note that the pressure does not appear in the above algorithm, however, by eliminating $\tilde{\mathbf{u}}^{n+1}$ from (2.2) using (2.4) and (2.8), we can obtain a pressure approximation

$$p^{n+1}=-\frac{1}{\tau}\phi^{n+1}+\mu s^{n+1}. \tag{2.9}$$

Next, we consider the stability of Algorithm 2.1. For the sake of simplicity, we assume o homogeneous Dirichlet boundary conditions for velocity, i.e., $\mathbf{u}|_\Gamma=0$.

Theorem 2.1. *Assuming $\mathbf{g}_1\equiv0$, the Gauge–Uzawa Algorithm 2.1 is unconditionally stable in the sense that, for all $\tau>0$ and $0\le N\le T_1/\tau-1$, the following a priori bounds hold:*

$$\|\rho^{N+1}\|_0^2+\sum_{n=0}^{N}\|\rho^{n+1}-\rho^n\|_0^2=\|\rho^0\|_0^2, \tag{2.10}$$

$$\begin{aligned}&\|\sigma^{N+1}\tilde{\mathbf{u}}^{N+1}\|_0^2+\sum_{n=0}^{N}(\|\sigma^{n+1}\tilde{\mathbf{u}}^{n+1}-\sigma^n\mathbf{u}^n\|_0^2+\|\frac{1}{\sigma^n}\nabla\phi^n\|_0^2)+\mu\tau\|s^{N+1}\|_0^2+\frac{\mu}{2}\tau\sum_{n=0}^{N}\|\nabla\tilde{\mathbf{u}}^{n+1}\|_0^2\\&\quad\le\|\sigma^0\tilde{\mathbf{u}}^0\|_0^2+CT_1\|\rho^0\|_0^2,\end{aligned} \tag{2.11}$$

and

$$\|\sigma^{N+1}T^{N+1}\|_0^2+\sum_{n=0}^{N}\|\sigma^{n+1}T^{n+1}-\sigma^nT^n\|_0^2+2\kappa\tau\sum_{n=0}^{N}\|\nabla T^{n+1}\|_0^2=\|\sigma^0T^0\|_0^2. \tag{2.12}$$

Proof. Taking the inner product of (2.1) with $2\tau\rho^{n+1}$ and using the identity (1.5a), we obtain

$$\|\rho^{n+1}\|_0^2 + \|\rho^{n+1} - \rho^n\|_0^2 - \|\rho^n\|_0^2 = 0. \tag{2.13}$$

Summing up the above for n from 0 to N leads to (2.10).

Then we take the inner product of (2.2) with $2\tau\tilde{\mathbf{u}}^{n+1}$, thanks to (1.5b), we get

$$\|\sigma^{n+1}\tilde{\mathbf{u}}^{n+1}\|_0^2 + \|\sigma^{n+1}\tilde{\mathbf{u}}^{n+1} - \sigma^n\mathbf{u}^n\|_0^2 - \|\sigma^n\mathbf{u}^n\|_0^2 + 2\mu\tau\|\nabla\tilde{\mathbf{u}}^{n+1}\|_0^2 + 2\mu\tau\langle\nabla s^n, \tilde{\mathbf{u}}^{n+1}\rangle = 2\tau(\rho^{n+1}\mathbf{g}, \tilde{\mathbf{u}}^{n+1}). \tag{2.14}$$

The next task is to derive a suitable relation between $\|\sigma^n\mathbf{u}^n\|_0^2$ and $\|\sigma^n\tilde{\mathbf{u}}^n\|_0^2$ so that we can sum up (2.14) over n. We derive from (2.3) and (2.7) that

$$\begin{aligned}\|\sigma^n\mathbf{u}^n\|_0^2 &= \langle\rho^n\mathbf{u}^n, \mathbf{u}^n\rangle = \langle\rho^n\tilde{\mathbf{u}}^n + \nabla\phi^n, \mathbf{u}^n\rangle = \langle\rho^n\tilde{\mathbf{u}}^n, \mathbf{u}^n\rangle = \left\langle\rho^n\tilde{\mathbf{u}}^n, \tilde{\mathbf{u}}^n + \frac{1}{\rho^n}\nabla\phi^n\right\rangle \\ &= \|\sigma^n\tilde{\mathbf{u}}^n\|_0^2 + \left\langle\mathbf{u}^n - \frac{1}{\rho^n}\nabla\phi^n, \nabla\phi^n\right\rangle = \|\sigma^n\tilde{\mathbf{u}}^n\|_0^2 - \|\frac{1}{\sigma^n}\nabla\phi^n\|_0^2.\end{aligned} \tag{2.15}$$

Now, we sum up (2.14) and (2.15) to get

$$\|\sigma^{n+1}\tilde{\mathbf{u}}^{n+1}\|_0^2 - \|\sigma^n\tilde{\mathbf{u}}^n\|_0^2 + \|\sigma^{n+1}\mathbf{u}^{n+1} - \sigma^n\tilde{\mathbf{u}}^n\|_0^2 + \|\frac{1}{\sigma^n}\nabla\phi^n\|_0^2 + 2\mu\tau\|\nabla\tilde{\mathbf{u}}^{n+1}\|_0^2 = A_1 + A_2 \tag{2.16}$$

with

$$A_1 := 2\mu\tau\langle s^n, \nabla\cdot\tilde{\mathbf{u}}^{n+1}\rangle,\ A_2 := 2\tau\langle\rho^{n+1}\mathbf{g}, \tilde{\mathbf{u}}^{n+1}\rangle. \tag{2.17}$$

We derive from the well-known inequality

$$\|\nabla\cdot\mathbf{v}\|_0 \le \|\nabla\mathbf{v}\|_0, \quad \forall\mathbf{v}\in\mathbf{H}_0^1(\Omega),\ \ d\ge 2, \tag{2.18}$$

and (2.4) that

$$\begin{aligned}A_1 &= -2\mu\tau\langle s^n, s^{n+1} - s^n\rangle = -\mu\tau(\|s^{n+1}\|_0^2 - \|s^n - s^{n+1}\|_0^2 - \|s^n\|_0^2) \\ &= -\mu\tau(\|s^{n+1}\|_0^2 - \|s^n\|_0^2) + \mu\tau\|\nabla\cdot\tilde{\mathbf{u}}^{n+1}\|_0^2 \\ &\le -\mu\tau(\|s^{n+1}\|_0^2 - \|s^n\|_0^2) + \mu\tau\|\nabla\tilde{\mathbf{u}}^{n+1}\|_0^2.\end{aligned} \tag{2.19}$$

On the other hand, using the Cauchy–Schwarz inequality and $\|\mathbf{v}\|_0 \le C\|\nabla\mathbf{v}\|_0$ ($\forall\mathbf{v}\in\mathbf{H}_0^1(\Omega)$), we obtain

$$\begin{aligned}A_2 &\le 2\tau\|\mathbf{g}\|_0\|\rho^{n+1}\|_0\|\tilde{\mathbf{u}}^{n+1}\|_0 \le 2C\tau\|\mathbf{g}\|_0\|\rho^{n+1}\|_0\|\nabla\tilde{\mathbf{u}}^{n+1}\|_0 \\ &\le C\tau\|\rho^{n+1}\|_0^2 + \frac{\mu}{2}\tau\|\nabla\tilde{\mathbf{u}}^{n+1}\|_0^2\end{aligned} \tag{2.20}$$

where C depends on μ, $\mathbf{g}$. From (2.13), we have

$$\|\rho^{n+1}\|_0^2 \le \|\rho^n\|_0^2 \le \|\rho^0\|_0^2. \tag{2.21}$$

Thus, we derive from (2.20) and (2.21) that

$$A_2 \le C\tau\|\rho^0\|_0^2 + \frac{\mu}{2}\tau\|\nabla\tilde{\mathbf{u}}^{n+1}\|_0^2. \tag{2.22}$$

Inserting (2.19) and (2.22) into (2.16) leads to

$$\begin{aligned}&\|\sigma^{n+1}\tilde{\mathbf{u}}^{n+1}\|_0^2 - \|\sigma^n\tilde{\mathbf{u}}^n\|_0^2 + \|\sigma^{n+1}\mathbf{u}^{n+1} - \sigma^n\tilde{\mathbf{u}}^n\|_0^2 + \mu\tau(\|s^{n+1}\|_0^2 - \|s^n\|_0^2) \\ &\quad + \|\frac{1}{\sigma^n}\nabla\phi^n\|_0^2 + \frac{\mu}{2}\tau\|\nabla\tilde{\mathbf{u}}^{n+1}\|_0^2 \le C\tau\|\rho^0\|_0^2.\end{aligned} \tag{2.23}$$

Summing (2.23) over n from 0 to N yields (2.11).

Finally, taking the inner product of (2.5) with $2\tau T^{n+1}$, thanks to (1.5c), we obtain

$$\|\sigma^{n+1}T^{n+1}\|_0^2 - \|\sigma^nT^n\|_0^2 + \|\sigma^{n+1}T^{n+1} - \sigma^nT^n\|_0^2 + 2\kappa\tau\|\nabla T^{n+1}\|_0^2 = 0. \tag{2.24}$$

Summing it over n from 0 to N leads to (2.12). The proof is complete. □

2.2. Gauge–Uzawa FEM and its stability: full discretization

In this subsection, we introduce a spatial discretization of Algorithm 2.1 for NC equations with variable density. Let $\mathcal{T}_h = \{K\}$ be a uniformly regular family of triangulation of Ω, and define the mesh size $h = \max_{K\in\mathcal{T}_h}\{\mathrm{diam}(K)\}$. The spatial approximation of fluid density, velocity, hydrodynamic pressure and temperature field is applied by mixed element method with $(M_h, \mathbf{X}_h, Q_h, W_h)$. Next, we present the following discrete subspaces:

$$
\begin{aligned}
&M_h = \Big\{\psi_h \in L^2(\Omega) : \psi_h|_K \in P_2(K),\ \ \forall K \in \mathcal{T}_h\Big\},\\
&\mathbf{V}_h^{\mathbf{b}} = \Big\{\mathbf{v}_h \in \mathbf{C}(\bar{\Omega}) : \mathbf{v}_h|_K \in (P_2(K))^2,\ \ \forall K \in \mathcal{T}_h; \mathbf{v}_h|_\Gamma = \mathbf{b}\Big\},\\
&Q_h = \Big\{q_h \in L^2(\Omega)\cap C(\bar{\Omega}) : q_h|_K \in P_1(K),\ \ \forall K \in \mathcal{T}_h\Big\},\\
&W_h = \Big\{s_h \in C(\bar{\Omega}) : s_h|_K \in P_2(K),\ \ \forall K \in \mathcal{T}_h\Big\},\\
&\mathbf{X}_h = \mathbf{V}_h^{\mathbf{b}} + \nabla Q_h,
\end{aligned}
$$

where $P_i(K)$ is the set of all polynomials on K of degree less than or equal to $i \in \mathbb{N}$, $\mathbf{b}$ is boundary condition. Then, the Gauge–Uzawa finite element method (FEM) reads as follows.

Algorithm 2.2 *(Gauge–Uzawa FEM).* Let ρ_{0h}, $\mathbf{u}_{0h}$ and T_{0h} be a suitable approximation of ρ_0, $\mathbf{u}_0$ and T_0, respectively. Set $\rho_h^0 = \rho_{0h}$, $\mathbf{u}_h^0 = \mathbf{u}_{0h}$, $T_h^0 = T_{0h}$ and $s_h^0 = 0$; repeat for $1 \le n \le N$:

Step 1. Find $\rho_h^{n+1} \in M_h$ for $\forall \psi_h \in M_h$ such that

$$
\left\langle \frac{\rho_h^{n+1} - \rho_h^n}{\tau} + \mathbf{u}_h^n \cdot \nabla \rho_h^{n+1} + \frac{\rho_h^{n+1}}{2}\nabla\cdot\mathbf{u}_h^n, \psi_h \right\rangle = 0. \tag{2.25}
$$

Step 2. Find $\tilde{\mathbf{u}}_h^{n+1} \in \mathbf{V}_h^{\mathbf{g}_1^{n+1}}$ for $\forall \mathbf{v}_h \in \mathbf{V}_h^0$ such that

$$
\begin{aligned}
&\left\langle \sigma_h^{n+1}\frac{\sigma_h^{n+1}\tilde{\mathbf{u}}_h^{n+1} - \sigma_h^n\mathbf{u}_h^n}{\tau}, \mathbf{v}_h \right\rangle + \left\langle \rho_h^{n+1}(\mathbf{u}_h^n\cdot\nabla)\tilde{\mathbf{u}}_h^{n+1}, \mathbf{v}_h\right\rangle + \left\langle \frac{1}{2}(\mathbf{u}_h^n\cdot\nabla\rho_h^{n+1})\tilde{\mathbf{u}}_h^{n+1}, \mathbf{v}_h\right\rangle\\
&\qquad + \mu\left\langle \nabla s_h^n, \nabla\cdot\mathbf{v}_h\right\rangle - \mu\left\langle \nabla\tilde{\mathbf{u}}_h^{n+1}, \nabla\tilde{\mathbf{v}}_h^{n+1}\right\rangle = \left\langle \rho_h^{n+1}\mathbf{g}, \mathbf{v}_h\right\rangle.
\end{aligned} \tag{2.26}
$$

Step 3. Find $\phi_h^{n+1} \in Q_h$ for $\forall q_h \in Q_h$ such that

$$
\left\langle \frac{1}{\rho_h^{n+1}}\nabla\phi_h^{n+1}, \nabla q_h\right\rangle = -\left\langle \tilde{\mathbf{u}}_h^{n+1}, \nabla q_h\right\rangle. \tag{2.27}
$$

Step 4. Update $\mathbf{u}_h^{n+1}$ and $s_h^{n+1} \in Q_h$ by

$$
\begin{cases}
\mathbf{u}_h^{n+1} = \tilde{\mathbf{u}}_h^{n+1} + \dfrac{1}{\rho_h^{n+1}}\nabla\phi_h^{n+1},\\
\left\langle s_h^{n+1}, q_h\right\rangle = \left\langle s_h^n - \nabla\cdot\tilde{\mathbf{u}}_h^{n+1}, q_h\right\rangle, \quad \forall q_h \in Q_h.
\end{cases} \tag{2.28}
$$

Step 5. Find T_h^{n+1} for $\forall \varphi_h \in W_h$ such that

$$
\left\langle \sigma_h^{n+1}\frac{\sigma_h^{n+1}T_h^{n+1} - \sigma_h^n T_h^n}{\tau}, \varphi_h\right\rangle + \left\langle \rho_h^{n+1}(\mathbf{u}_h^{n+1}\cdot\nabla)T_h^{n+1}, \varphi_h\right\rangle + \kappa\left\langle \nabla T_h^{n+1}, \nabla\varphi_h\right\rangle + \frac{1}{2}\left\langle (\mathbf{u}_h^{n+1}\cdot\nabla\rho_h^{n+1})T_h^{n+1}, \varphi_h\right\rangle = 0. \tag{2.29}
$$

Theorem 2.2. *Assuming $\mathbf{g}_1 \equiv 0$, the Gauge–Uzawa Algorithm 2.2 is unconditionally stable in the sense that, for all $\tau > 0$ and $0 \le N \le T_1/\tau - 1$, the following a priori bounds hold:*

$$
\begin{aligned}
&\|\rho_h^{N+1}\|_0^2 + \sum_{n=0}^{N}\|\rho_h^{n+1} - \rho_h^n\|_0^2 = \|\rho_h^0\|_0^2,\\
&\|\sigma_h^{N+1}\tilde{\mathbf{u}}_h^{N+1}\|_0^2 + \sum_{n=0}^{N}(\|\sigma_h^{n+1}\tilde{\mathbf{u}}_h^{n+1} - \sigma_h^n\mathbf{u}_h^n\|_0^2 + \|\frac{1}{\sigma_h^n}\nabla\phi_h^n\|_0^2) + \mu\tau\|s_h^{N+1}\|_0^2 + \frac{\mu}{2}\tau\sum_{n=0}^{N}\|\nabla\tilde{\mathbf{u}}_h^{n+1}\|_0^2\\
&\quad \le \|\sigma_h^0\tilde{\mathbf{u}}_h^0\|_0^2 + CT_1\|\rho_h^0\|_0^2,
\end{aligned}
$$

and

$$\|\sigma_h^{N+1}T_h^{N+1}\|_0^2+\sum_{n=0}^{N}\|\sigma_h^{n+1}T_h^{n+1}-\sigma_h^nT_h^n\|_0^2+2\kappa\tau\sum_{n=0}^{N}\|\nabla T_h^{n+1}\|_0^2=\|\sigma_h^0T_h^0\|_0^2.$$

Proof. We can prove the desired result by using exactly the same procedure as in the proof of Theorem 2.1. Note that while $\nabla\cdot\mathbf{u}_h^{n+1}$ is not necessarily zero, we can derive from (2.28) and (2.29) that $\langle\mathbf{u}_h^{n+1},\nabla q_h\rangle=0$, $\forall q_h\in Q_h$ which is a discrete counterpart of (2.7). □

2.3. Second-order Gauge–Uzawa scheme

Algorithm 2.1 is only first-order accurate. However, a second-order version with essentially the same computational procedures can be constructed as follows. For simplicity, we denote, for any function a, its second-order extrapolation by $\bar{a}^{n+1}=2a^n-a^{n-1}$.

Algorithm 2.3 *(Second-order Gauge–Uzawa method).* Set $\rho^0=\rho_0$, $\mathbf{u}^0=\mathbf{u}_0$, $T^0=T_0$ and $s^0=0$ and compute ρ^1, $\mathbf{u}^1$, p^1, s^1 with Algorithm 2.1, then repeat for $2\le n\le N$.

Step 1. Find ρ^{n+1} as the solution of

$$\begin{cases}\dfrac{3\rho^{n+1}-4\rho^n+\rho^{n-1}}{2\tau}+\bar{\mathbf{u}}^{n+1}\cdot\nabla\rho^{n+1}+\dfrac{\rho^{n+1}}{2}\nabla\cdot\bar{\mathbf{u}}^{n+1}=0,\\ \rho^{n+1}|_{\Gamma_{\bar{\mathbf{u}}^{n+1}}}=r^{n+1}.\end{cases}\tag{2.30}$$

Step 2. Find $\tilde{\mathbf{u}}^{n+1}$ as the solution of

$$\begin{cases}\rho^{n+1}\dfrac{3\tilde{\mathbf{u}}^{n+1}-4\mathbf{u}^n+\mathbf{u}^{n-1}}{2\tau}+\rho^{n+1}(\bar{\mathbf{u}}^{n+1}\cdot\nabla)\tilde{\mathbf{u}}^{n+1}+\dfrac{\tilde{\mathbf{u}}^{n+1}}{2}(\bar{\mathbf{u}}^{n+1}\cdot\nabla\rho^{n+1})\\ \qquad\qquad+\nabla p^n+\mu\nabla s^n-\mu\Delta\tilde{\mathbf{u}}^{n+1}=\rho^{n+1}\mathbf{g},\\ \tilde{\mathbf{u}}^{n+1}|_\Gamma=\mathbf{g}_1^{n+1}.\end{cases}\tag{2.31}$$

Step 3. Find ϕ^{n+1} as the solution of

$$\begin{cases}-\nabla\cdot(\dfrac{1}{\rho^{n+1}}\nabla\phi^{n+1})=\nabla\cdot\tilde{\mathbf{u}}^{n+1},\\ \partial_{\mathbf{n}}\phi^{n+1}|_\Gamma=0.\end{cases}\tag{2.32}$$

Step 4. Update $\mathbf{u}^{n+1}$ and s^{n+1} by

$$\begin{cases}\mathbf{u}^{n+1}=\tilde{\mathbf{u}}^{n+1}+\dfrac{1}{\rho^{n+1}}\nabla\phi^{n+1},\\ s^{n+1}=s^n-\nabla\cdot\tilde{\mathbf{u}}^{n+1},\\ p^{n+1}=p^n-\dfrac{3\phi^{n+1}}{2\tau}+\mu s^{n+1}.\end{cases}\tag{2.33}$$

Step 5. Find T^{n+1} as the solution of

$$\begin{cases}\rho^{n+1}\dfrac{3T^{n+1}-4T^n+T^{n-1}}{2\tau}+\rho^{n+1}(\bar{\mathbf{u}}^{n+1}\cdot\nabla)T^{n+1}+\dfrac{T^{n+1}}{2}(\bar{\mathbf{u}}^{n+1}\cdot\nabla\rho^{n+1})-\kappa\Delta T^{n+1}=0,\\ T^{n+1}|_\Gamma=g_2^{n+1}.\end{cases}\tag{2.34}$$

Similarly, we can construct fully-discrete version of Algorithm 2.3.

Remark 2.3. Although numerical experiments indicate that this scheme is unconditionally stable, how to prove the stability of Algorithm 2.3 is still an open problem. In fact, to the best of the authors' knowledge, there is no provably stable second-order projection type scheme available even for the variable density Navier–Stokes equations.

3. Gauge–Uzawa methods in convective form

We construct in this section Gauge–Uzawa methods in convective form which is more convenient for non-variational methods such as spectral-collocation method or finite difference method.

3.1. First-order Gauge–Uzawa method

Algorithm 3.1 *(Gauge–Uzawa method in convective form).* Given $\rho^0 = \rho_0$, $\mathbf{u}^0 = \mathbf{u}_0$, $T^0 = T_0$, and $s^0 = 0$, then repeat the following steps for $1 \le n \le N$:

Step 1. Find ρ^{n+1} as the solution of

$$\begin{cases} \dfrac{\rho^{n+1} - \rho^n}{\tau} + \mathbf{u}^n \cdot \nabla \rho^{n+1} = 0, \\ \rho^{n+1}|_{\Gamma_{\mathbf{u}^n}} = r^{n+1}. \end{cases} \tag{3.1}$$

Step 2. Find $\tilde{\mathbf{u}}^{n+1}$ as the solution of

$$\begin{cases} \rho^n \dfrac{\tilde{\mathbf{u}}^{n+1} - \mathbf{u}^n}{\tau} + \rho^{n+1}(\mathbf{u}^n \cdot \nabla)\tilde{\mathbf{u}}^{n+1} + \mu \nabla s^n - \mu \Delta \tilde{\mathbf{u}}^{n+1} = \rho^{n+1}\mathbf{g}, \\ \tilde{\mathbf{u}}^{n+1}|_\Gamma = \mathbf{g}_1^{n+1}. \end{cases} \tag{3.2}$$

Step 3. Find ϕ^{n+1} as the solution of

$$\begin{cases} -\nabla \cdot \left(\dfrac{1}{\rho^{n+1}} \nabla \phi^{n+1}\right) = \nabla \cdot \tilde{\mathbf{u}}^{n+1}, \\ \partial_{\mathbf{n}} \phi^{n+1}|_\Gamma = 0. \end{cases} \tag{3.3}$$

Step 4. Update $\mathbf{u}^{n+1}$ and s^{n+1} by

$$\begin{cases} \mathbf{u}^{n+1} = \tilde{\mathbf{u}}^{n+1} + \dfrac{1}{\rho^{n+1}} \nabla \phi^{n+1}, \\ s^{n+1} = s^n - \nabla \cdot \tilde{\mathbf{u}}^{n+1}. \end{cases} \tag{3.4}$$

Step 5. Find T^{n+1} as the solution of

$$\begin{cases} \rho^n \dfrac{T^{n+1} - T^n}{\tau} + \rho^{n+1}(\mathbf{u}^n \cdot \nabla) T^{n+1} - \kappa \Delta T^{n+1} = 0, \\ T^{n+1}|_\Gamma = g_2^{n+1}. \end{cases} \tag{3.5}$$

Remark 3.1. In this Algorithm, the pressure does not appear explicitly but its approximation can be defined by (2.9). Fully-discrete and second-order versions of Algorithm 3.1 can be similarly constructed as in Algorithm 2.2 and Algorithm 2.3, respectively.

Theorem 3.1. *Assuming $\mathbf{g}_1 \equiv 0$, the Gauge–Uzawa Algorithm 3.1 is unconditionally stable in the sense that, for all $\tau > 0$ and $0 \le N \le T_1/\tau - 1$, the following a priori bounds hold:*

$$\|\rho^{N+1}\|_0^2 + \sum_{n=0}^{N} \|\rho^{n+1} - \rho^n\|_0^2 = \|\rho^0\|_0^2, \tag{3.6}$$

$$\begin{aligned} &\|\sigma^{N+1}\tilde{\mathbf{u}}^{N+1}\|_0^2 + \sum_{n=0}^{N} \left(\|\sigma^n(\tilde{\mathbf{u}}^{n+1} - \mathbf{u}^n)\|_0^2 + \|\frac{1}{\sigma^n}\nabla\phi^n\|_0^2 \right) + \mu\tau\|s^{N+1}\|_0^2 + \frac{\mu}{2}\tau \sum_{n=0}^{N} \|\nabla \tilde{\mathbf{u}}^{n+1}\|_0^2 \\ &\quad \le \|\sigma^0 \tilde{\mathbf{u}}^0\|_0^2 + CT_1\|\rho^0\|_0^2, \end{aligned} \tag{3.7}$$

and

$$\|\sigma^{N+1}T^{N+1}\|_0^2 + \sum_{n=0}^{N} \|\sigma^{n+1}T^{n+1} - \sigma^n T^n\|_0^2 + 2\kappa\tau \sum_{n=0}^{N} \|\nabla T^{n+1}\|_0^2 = \|\sigma^0 T^0\|_0^2. \tag{3.8}$$

Proof. Taking the inner product of (3.1) with $2\tau\rho^{n+1}$, thanks to the first equation in (1.5a), we get

$$\|\rho^{n+1}\|_0^2 + \|\rho^{n+1} - \rho^n\|_0^2 - \|\rho^n\|_0^2 = 0. \tag{3.9}$$

Summing up over n from 0 to N leads to (3.6).

Next, taking the inner product of (3.2) with $2\tau\tilde{\mathbf{u}}^{n+1}$, we find

$$2\langle\rho^n(\tilde{\mathbf{u}}^{n+1}-\mathbf{u}^n),\tilde{\mathbf{u}}^{n+1}\rangle+2\tau\langle\rho^{n+1}(\mathbf{u}^n\cdot\nabla)\tilde{\mathbf{u}}^{n+1},\tilde{\mathbf{u}}^{n+1}\rangle+2\mu\tau\langle\nabla s^n,\tilde{\mathbf{u}}^{n+1}\rangle+2\mu\tau\|\nabla\tilde{\mathbf{u}}^{n+1}\|_0^2=2\tau\langle\rho^{n+1}\mathbf{g},\tilde{\mathbf{u}}^{n+1}\rangle. \quad (3.10)$$

Now, we can write the first term in the above as

$$2\langle\rho^n(\tilde{\mathbf{u}}^{n+1}-\mathbf{u}^n),\tilde{\mathbf{u}}^{n+1}\rangle=\|\sigma^n\tilde{\mathbf{u}}^{n+1}\|_0^2+\|\sigma^n(\tilde{\mathbf{u}}^{n+1}-\mathbf{u}^n)\|_0^2-\|\sigma^n\mathbf{u}^n\|_0^2. \quad (3.11)$$

The relation (2.15) is still valid because we only used (2.3) and (2.7) to derive it. Hence, we only need to derive a suitable relation between $\|\sigma^n\tilde{\mathbf{u}}^{n+1}\|_0^2$ and $\|\sigma^{n+1}\tilde{\mathbf{u}}^{n+1}\|_0^2$. For this purpose, we take the inner product of (3.1) with a scalar function $\tau\tilde{\mathbf{u}}^{n+1}\cdot\tilde{\mathbf{u}}^{n+1}$ to get

$$\langle\rho^{n+1}-\rho^n,\tilde{\mathbf{u}}^{n+1}\cdot\tilde{\mathbf{u}}^{n+1}\rangle=-\tau\langle\nabla\cdot(\rho^{n+1}\mathbf{u}^n),\tilde{\mathbf{u}}^{n+1}\cdot\tilde{\mathbf{u}}^{n+1}\rangle, \quad (3.12)$$

which can be rewritten as

$$\|\sigma^{n+1}\tilde{\mathbf{u}}^{n+1}\|_0^2-\|\sigma^n\tilde{\mathbf{u}}^{n+1}\|_0^2=2\tau\langle\rho^{n+1}(\mathbf{u}^n\cdot\nabla)\tilde{\mathbf{u}}^{n+1},\tilde{\mathbf{u}}^{n+1}\rangle. \quad (3.13)$$

Combining (3.13) and (2.15) into (3.11), we obtain

$$\begin{aligned}&2\langle\rho^n(\tilde{\mathbf{u}}^{n+1}-\mathbf{u}^n),\tilde{\mathbf{u}}^{n+1}\rangle+2\tau\langle\rho^{n+1}(\mathbf{u}^n\cdot\nabla)\tilde{\mathbf{u}}^{n+1},\tilde{\mathbf{u}}^{n+1}\rangle\\&\quad=\|\sigma^{n+1}\tilde{\mathbf{u}}^{n+1}\|_0^2+\|\sigma^n(\tilde{\mathbf{u}}^{n+1}-\mathbf{u}^n)\|_0^2-\|\sigma^n\tilde{\mathbf{u}}^n\|_0^2+\|\frac{1}{\sigma^n}\nabla\phi^n\|_0^2.\end{aligned} \quad (3.14)$$

Then, we can derive from (3.10) and (3.14) that

$$\|\sigma^{n+1}\tilde{\mathbf{u}}^{n+1}\|_0^2+\|\sigma^n(\tilde{\mathbf{u}}^{n+1}-\mathbf{u}^n)\|_0^2-\|\sigma^n\tilde{\mathbf{u}}^n\|_0^2+\|\frac{1}{\sigma^n}\nabla\phi^n\|_0^2+2\mu\tau\|\nabla\tilde{\mathbf{u}}^{n+1}\|_0^2=A_1+A_2$$

with A_1 and A_2 defined in (2.17). Using the estimates (2.19) and (2.20) yields

$$\|\sigma^{n+1}\tilde{\mathbf{u}}^{n+1}\|_0^2-\|\sigma^n\tilde{\mathbf{u}}^n\|_0^2+\|\sigma^n(\mathbf{u}^{n+1}-\tilde{\mathbf{u}}^n)\|_0^2+\mu\tau(\|s^{n+1}\|_0^2-\|s^n\|_0^2)+\|\frac{1}{\sigma^n}\nabla\phi^n\|_0^2+\frac{\mu}{2}\tau\|\nabla\tilde{\mathbf{u}}^{n+1}\|_0^2\le C\tau\|\rho^0\|_0^2. \quad (3.15)$$

Summing up the above over n from 0 to N leads to (3.7).

Lastly, taking the inner product of (3.1) with a scalar function $\tau T^{n+1}T^{n+1}$ to get

$$\langle\rho^{n+1}-\rho^n,T^{n+1}T^{n+1}\rangle=-\tau\langle\nabla\cdot(\rho^{n+1}\mathbf{u}^n),T^{n+1}T^{n+1}\rangle, \quad (3.16)$$

which can be rewritten as

$$\|\sigma^{n+1}T^{n+1}\|_0^2-\|\sigma^nT^{n+1}\|_0^2=2\tau\langle\rho^{n+1}(\mathbf{u}^n\cdot\nabla)T^{n+1},T^{n+1}\rangle. \quad (3.17)$$

Taking the inner product of (3.5) with $2\tau T^{n+1}$ and using (3.17), we can get

$$\|\sigma^{n+1}T^{n+1}\|_0^2-\|\sigma^nT^n\|_0^2+\|\sigma^n(T^{n+1}-T^n)\|_0^2+\kappa\|\nabla T^{n+1}\|_0^2=0. \quad (3.18)$$

Summing up the above n from 0 to N leads to (3.8). The proof is complete. □

4. Numerical experiments

We present in this section some numerical experiments to validate the effectiveness of Gauge–Uzawa methods for NC problems. Throughout this section, we use the finite element spaces (P_2,P_2,P_1,P_2) for $(\rho,\mathbf{u},p,T)$.

Firstly, we consider a flow problem with manufactured analytical solution. Secondly, a Bénard convection problem is presented.

4.1. Examples with analytical solution

As a first example, in order to test the accuracy of algorithms proposed in this paper, we consider a known analytical solution:

$$\begin{aligned}&\rho(x_1,x_2,t)=2+x_1\cos(\sin(t))+x_2\sin(\sin(t)),\\&u_1(x_1,x_2,t)=-x_2\cos(t),\\&u_2(x_1,x_2,t)=x_1\cos(t),\\&p(x_1,x_2,t)=\sin(x_1)\sin(x_2)\sin(t),\\&T(x_1,x_2,t)=u_1(x_1,x_2,t)+u_2(x_1,x_2,t).\end{aligned}$$

Table 1
Error and convergence rate in time of the first-order Gauge–Uzawa method in conserved form.

τ	0.1	0.05	0.025	0.0125	0.00625	0.003125
$\frac{\|\nabla(\rho-\rho_h)\|_0}{\|\nabla\rho\|_0}$	8.7953E−1	4.4518E−1	2.2392E−1	1.1234E−1	5.6304E−2	2.8210E−2
Order	/	0.982	0.991	0.995	0.997	0.997
$\frac{\|\rho-\rho_h\|_0}{\|\rho\|_0}$	1.0194E−2	5.1668E−3	2.5998E−3	1.3038E−3	6.5288E−4	3.2668E−4
Order	/	0.980	0.991	0.996	0.998	0.999
$\frac{\|\nabla(u-u_h)\|_0}{\|\nabla u\|_0}$	3.8566E−2	1.8113E−2	8.7229E−3	4.2739E−3	2.1152E−3	1.0527E−3
Order	/	1.090	1.054	1.029	1.015	1.007
$\frac{\|u-u_h\|_0}{\|u\|_0}$	1.1796E−2	6.0288E−3	3.0390E−3	1.5246E−3	7.6342E−4	3.8197E−4
Order	/	0.968	0.988	0.995	0.998	0.999
$\frac{\|p-p_h\|_0}{\|p\|_0}$	2.6245E−1	1.3464E−1	6.8320E−2	3.4433E−2	1.7290E−2	8.6668E−3
Order	/	0.963	0.979	0.989	0.994	0.996
$\frac{\|\nabla(T-T_h)\|_0}{\|\nabla T\|_0}$	1.2806E−2	6.3355E−3	3.1499E−3	1.5704E−3	7.8404E−4	3.9173E−4
Order	/	1.015	1.008	1.004	1.002	1.001
$\frac{\|T-T_h\|_0}{\|T\|_0}$	6.2621E−3	3.1003E−3	1.5422E−3	7.6908E−4	3.8404E−4	1.9189E−4
Order	/	1.014	1.007	1.004	1.002	1.001
K_{div}	3.8140E−2	1.7001E−2	7.8937E−3	3.7836E−3	1.8510E−3	9.1680E−4
Order	/	1.166	1.107	1.061	1.032	1.014
$Error_{sum1}$	8.46512E−2	4.28300E−2	2.15485E−2	1.08085E−2	5.41295E−3	2.70866E−3
CPU(s)	273.88	529.90	1096.87	2197.47	4398.34	9275.64

Table 2
Error and convergence rate in time of the first-order Gauge–Uzawa method in convective form.

τ	0.1	0.05	0.025	0.0125	0.00625	0.003125
$\frac{\|\nabla(\rho-\rho_h)\|_0}{\|\nabla\rho\|_0}$	6.5886E−1	3.3523E−1	1.6924E−1	8.5069E−2	4.2658E−2	2.1362E−2
Order	/	0.975	0.986	0.992	0.996	0.998
$\frac{\|\rho-\rho_h\|_0}{\|\rho\|_0}$	1.0184E−2	5.1607E−3	2.5964E−3	1.3021E−3	6.5199E−4	3.2622E−4
Order	/	0.981	0.991	0.996	0.998	0.999
$\frac{\|\nabla(u-u_h)\|_0}{\|\nabla u\|_0}$	3.8605E−2	1.8141E−2	8.7382E−3	4.2818E−3	2.1192E−3	1.0548E−3
Order	/	1.090	1.054	1.029	1.015	1.007
$\frac{\|u-u_h\|_0}{\|u\|_0}$	1.1809E−2	6.0330E−3	3.0412E−3	1.5258E−3	7.6409E−4	3.8233E−4
Order	/	0.969	0.988	0.995	0.998	0.999
$\frac{\|p-p_h\|_0}{\|p\|_0}$	2.6147E−1	1.3420E−1	6.8115E−2	3.4335E−2	1.7242E−2	8.6424E−3
Order	/	0.962	0.978	0.988	0.994	0.996
$\frac{\|\nabla(T-T_h)\|_0}{\|\nabla T\|_0}$	1.2715E−2	6.3241E−3	3.1533E−3	1.5744E−3	7.8663E−4	3.9317E−4
Order	/	1.008	1.004	1.002	1.001	1.001
$\frac{\|T-T_h\|_0}{\|T\|_0}$	6.4481E−3	3.2211E−3	1.6098E−3	8.0470E−4	4.0230E−4	2.0113E−4
Order	/	1.001	1.001	1.000	1.000	1.000
K_{div}	3.8067E−2	1.6990E−2	7.8914E−3	3.7831E−3	1.8508E−3	9.1676E−4
Order	/	1.164	1.106	1.061	1.031	1.014
$Error_{sum2}$	8.46678E−2	4.28348E−2	2.15498E−2	1.08089E−2	5.41303E−3	2.70868E−3
CPU(s)	261.73	468.53	1026.36	1960.21	3680.27	8151.78

The computational domain is an unit circle. We choose $\mu = 1$, $\kappa = 1$, $T_1 = 1$, and the initial conditions in (1.1) are given by the above exact solutions.

The convergence rates with respect to the time step τ are calculated by the formula $\frac{\log(E_i/E_{i+1})}{\log(\tau_i/\tau_{i+1})}$, where E_i and E_{i+1} are the relative errors corresponding to the time steps τ_i and τ_{i+1}, respectively.

Computation are made on a fixed small enough mesh size with different time steps so that the error from the spatial discretization is negligible compared with the time error. The results are given in Tables 1–3, where $K_{div} = \max_{K_h(\Omega)} |\int_k \nabla\cdot\mathbf{u}_h dx|$, $Error_{sum1} = \sum_{n=0}^{N} \|\sigma^{n+1}\tilde{\mathbf{u}}^{n+1} - \sigma^n\mathbf{u}^n\|_0^2$ in (2.11), $Error_{sum2} = \sum_{n=0}^{N} \|\sigma^n(\tilde{\mathbf{u}}^{n+1} - \mathbf{u}^n)\|_0^2$ in (3.7). From Tables 1–2, we observe that the numerical results with the Gauge–Uzawa FEM in conserved and convective forms behave similarly, so we only present the numerical results of 2nd-order scheme in convective form in Table 3. These results indicate that first- and second-order convergence rates are achieved with the first- and second-order schemes, respectively. As for CPU time, we observe that the conserved scheme is slightly more expensive than the convective scheme.

4.2. Bénard convection

As the second example, we consider the Bénard convection which is a classical fluid dynamic phenomenon. In the standard case, the temperatures of the top and bottom plates are assumed to be distributed homogeneously.

Table 3
Error and convergence rate in time of the second-order Gauge–Uzawa method in convective form.

τ	1/10	1/20	1/30	1/40	1/50	1/60
$\frac{\|\nabla(\rho-\rho_h)\|_0}{\|\nabla\rho\|_0}$	1.4223E−1	3.7835E−2	1.7318E−2	9.9221E−3	6.4300E−3	4.5066E−3
Order	/	1.911	1.927	1.936	1.944	1.949
$\frac{\|\rho-\rho_h\|_0}{\|\rho\|_0}$	1.4328E−3	3.5278E−4	1.5583E−4	8.7363E−5	5.5795E−5	3.8690E−5
Order	/	2.022	2.015	2.012	2.009	2.008
$\frac{\|\nabla(u-u_h)\|_0}{\|\nabla u\|_0}$	6.6946E−3	1.6682E−3	7.4067E−4	4.1634E−4	2.6632E−4	1.8488E−4
Order	/	2.005	2.002	2.002	2.002	2.002
$\frac{\|u-u_h\|_0}{\|u\|_0}$	3.2855E−3	8.1434E−4	3.6073E−4	2.0252E−4	1.2945E−4	8.9820E−5
Order	/	2.012	2.008	2.007	2.006	2.005
$\frac{\|p-p_h\|_0}{\|p\|_0}$	4.7783E−2	1.1758E−2	5.2019E−3	2.9217E−3	1.8756E−3	1.3229E−3
Order	/	2.023	2.011	2.005	1.986	1.915
$\frac{\|\nabla(T-T_h)\|_0}{\|\nabla T\|_0}$	1.1530E−3	2.9041E−4	1.2965E−5	7.3101E−5	4.6853E−5	3.2568E−5
Order	/	1.989	1.989	1.992	1.994	1.995
$\frac{\|T-T_h\|_0}{\|T\|_0}$	6.5338E−3	1.6314E−4	7.2625E−5	4.0894E−5	2.6189E−5	1.8195E−5
Order	/	2.002	1.996	1.996	1.997	1.998
K_{div}	1.7081E−3	4.5968E−4	2.1219E−4	1.2162E−4	7.8734E−5	5.5153E−5
Order	/	1.894	1.907	1.935	1.949	1.952
CPU(s)	463.97	870.38	1292.39	1934.95	2345.98	2811.36

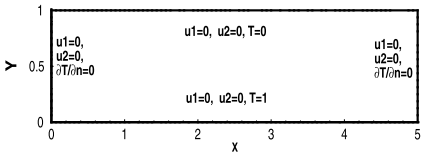

Fig. 1. Bénard Convection: domain and boundary conditions.

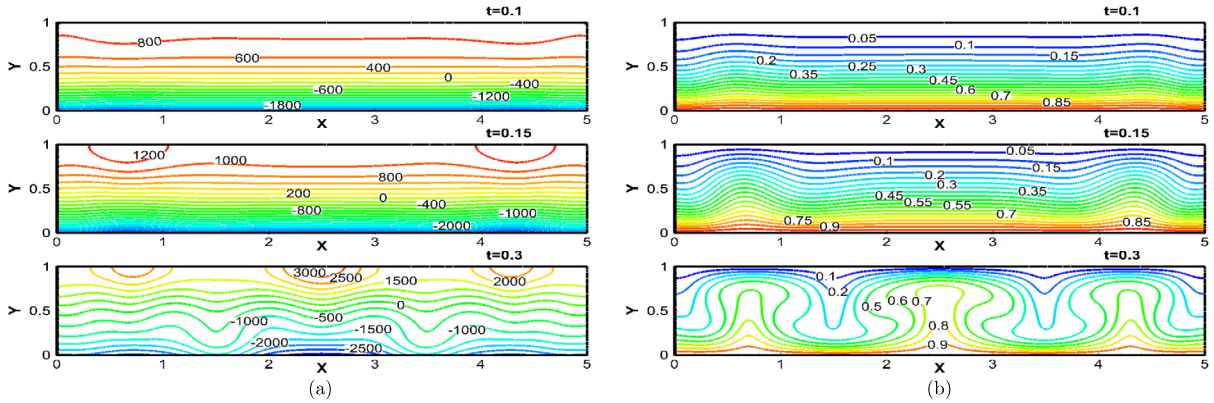

Fig. 2. Bénard convection based on Boussinesq approximation with $Pr = 1$, $Ra = 10^4$, $\tau = 0.01$, $h = 1/150$: (a) pressure; (b) temperature.

The domain and boundary conditions of Bénard convection problem are displayed in Fig. 1. The top boundary is isothermal and the bottom plate is uniformly heated; both vertical walls are adiabatic. And the boundary conditions for the velocity are no-slip at all boundaries. The initial conditions are $T^0 = 0$, $\mathbf{u}^0 = 0$ and $\rho^0 = 0.01 * (y + 1)$.

4.2.1. Boussinesq approximation

We first consider the natural convection with small density difference such that the well-known Boussinesq approximation can be used. In order to validate our methodology and compare with the data provided by [14,22], we consider the uniformly heated boundary condition on the bottom plate with $\kappa = 1$, $h = 1/150$, $Pr = 1$. Figs. 2–3 show the pressure, temperature and velocity fields of NC equations based on the Boussinesq approximation using the second-order Gauge–Uzawa FEM with $\nu = 1$, $Ra = 10^4$, $\tau = 0.01$ at times $t = 0.1$, $t = 0.15$, $t = 0.3$. And in Figs. 4–5 we present the numerical results with $\nu = 10$, $Ra = 10^6$, $\tau = 5 \times 10^{-5}$ at $t = 0.03$, $t = 0.05$, $t = 0.08$. We observe in particular appearance of the well documented convection rolls in Fig. 3 and Fig. 5, and more rolls appear as Ra increases.

4.2.2. Non-Boussinesq regime

In many applications such as geophysical flows, density varies significantly under the influence of temperature such that the Boussinesq approximation is no longer valid. In these cases, we use the model (1.1). Since the Rayleigh number

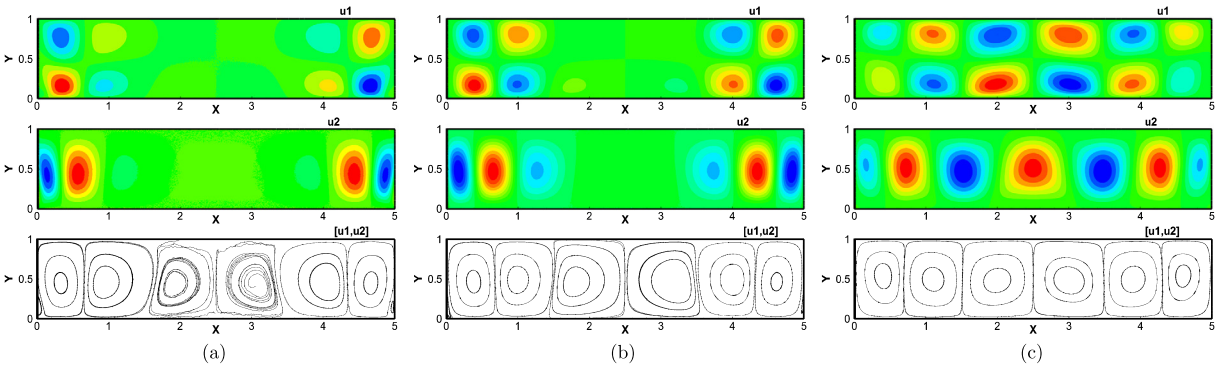

Fig. 3. Velocity of Bénard convection based on Boussinesq approximation at $\nu = 1$, $Pr = 1$, $Ra = 10^4$, $\kappa = 1$, $\tau = 0.01$, $h = 1/150$ at different times: (a) $t = 0.1$, (b) $t = 0.15$, (c) $t = 0.3$.

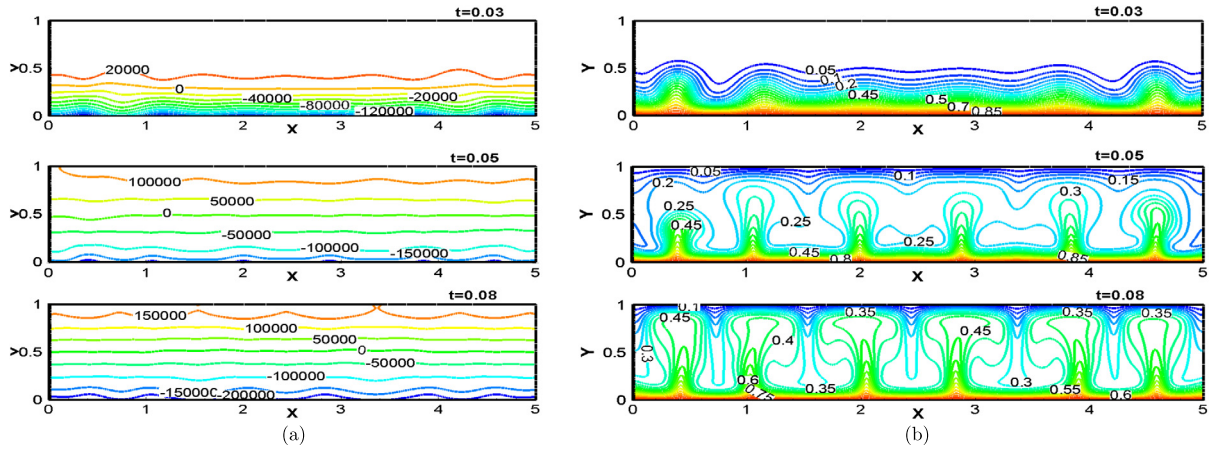

Fig. 4. Bénard convection based on Boussinesq approximation with $\nu = 10$, $Pr = 1$, $\kappa = 1$, $Ra = 10^6$, $\tau = 5 \times 10^{-5}$, $h = 1/150$: (a) pressure; (b) temperature.

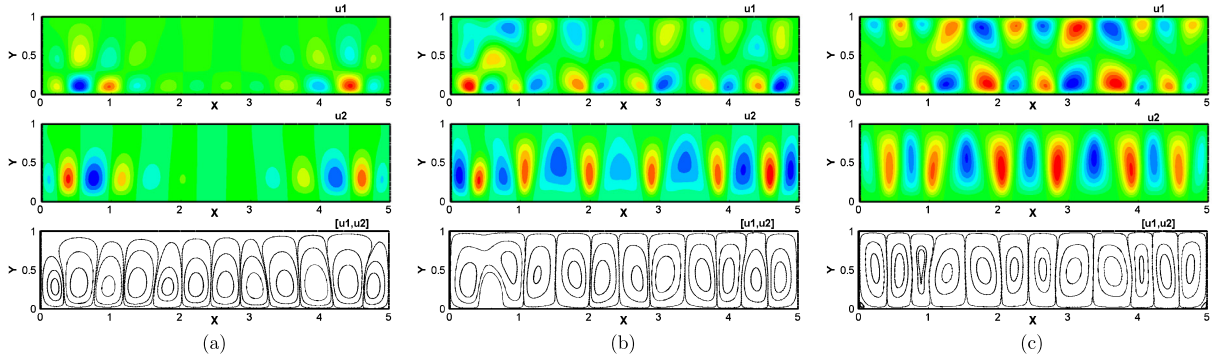

Fig. 5. Velocity of Bénard convection based on Boussinesq approximation at $\nu = 10$, $Pr = 1$, $Ra = 10^6$, $\kappa = 1$, $\tau = 5 \times 10^{-5}$, $h = 1/150$ at different times: (a) $t = 0.03$, (b) $t = 0.05$, (c) $t = 0.08$.

(Ra), which describes the relationship between buoyancy and viscosity within a fluid and can also be used as a criterion to predict convectional instabilities, is the most important dimensionless number for NC problem with small density variations, we introduce a similar dimensionless number (Ra_1) in the right hand side of (1.1b) to control the magnitude of buoyancy force for NC problem with large density variations.

We study below the influence of the ratio of μ (controlling the magnitude of viscosity force) and Ra_1. First, we take $Ra_1 = 10^4$, $\mu = 1$, $\kappa = 1$, $\tau = 10^{-3}$, $h = 1/100$. The density, temperature and streamline function by the 2nd-order scheme are shown in Fig. 6. In this case, $Ra_1/\mu = 10^4$ so heat transfer is primarily in the form of conduction. Hence, the isothermal lines and density contours nearly parallel to the bottom plate. Next, we choose $Ra_1 = 10^3$, $\mu = 0.01$, $\kappa = 0.01$, $\tau = 10^{-4}$, $h = 1/120$. The density, temperature and streamline functions by the 2nd-order scheme are shown in Fig. 7. Finally, we present in Figs. 8–9 the numerical results of the 2nd-order scheme at different times with $\nu = 1$, $Pr = 1$, $Ra_1 = 10^5$,

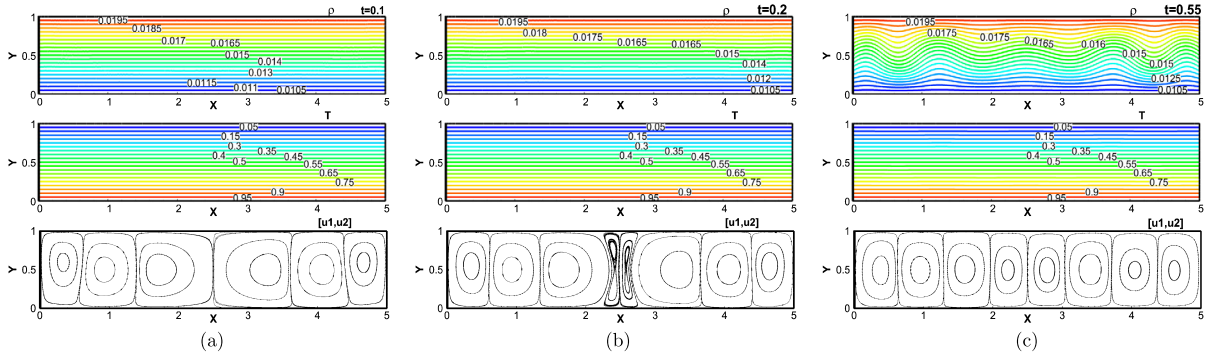

Fig. 6. Isolines of density, temperature and streamlines of velocity (from up to bottom) of Bénard convection problem with variable density with $\nu = 1$, $Pr = 1$, $Ra_1 = 10^4$, $\kappa = 1$, $\tau = 10^{-3}$, $h = 1/100$ by the second-order Gauge–Uzawa FEM at different time: (a) $t = 0.1$, (b) $t = 0.2$, (c) $t = 0.55$.

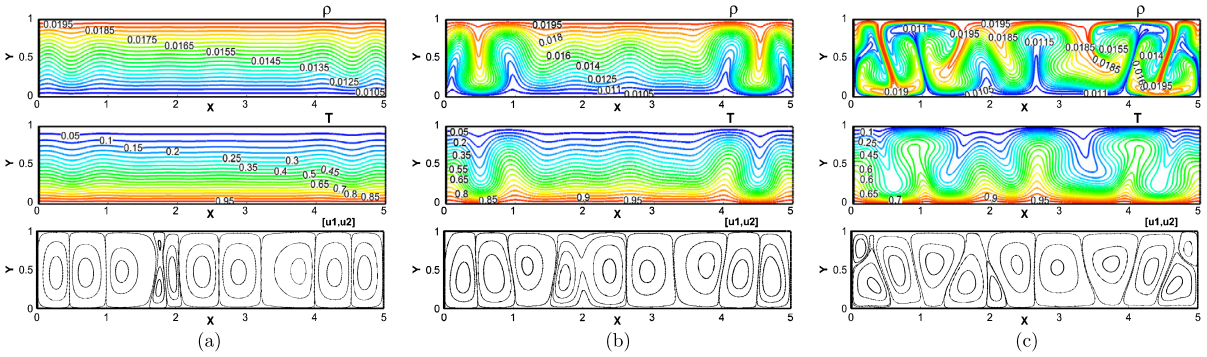

Fig. 7. Isolines of density, temperature and streamlines of velocity (from up to bottom) of Bénard convection problem with variable density with $\nu = 0.01$, $Pr = 1$, $Ra_1 = 10^3$, $\kappa = 0.01$, $\tau = 10^{-4}$, $h = 1/120$ by the second-order Gauge–Uzawa FEM at difference time: (a) $t = 0.2$, (b) $t = 0.24$, (c) $t = 0.28$.

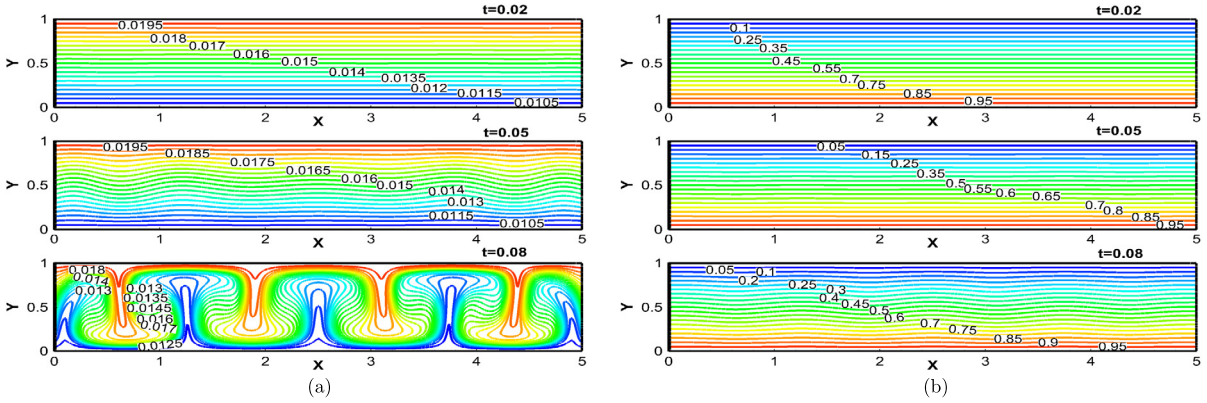

Fig. 8. Isolines of density (a) and temperature (b) of Bénard convection problem with variable density with $\nu = 1$, $Pr = 1$, $Ra_1 = 10^5$, $\kappa = 1$, $\tau = 10^{-4}$, $h = 1/120$ by the second-order Gauge–Uzawa FEM at difference time: $t = 0.02$, $t = 0.05$, $t = 0.08$ (from top to bottom).

$\kappa = 1$, $\tau = 10^{-4}$, $h = 1/120$. We observe from Figs. 7–9 that the heat transfer is primarily in the form of convection when $Ra_1/\mu = 10^5$. In these cases, a series of transitions to more complicated states occur. It is expected that the flow will eventually become turbulent when Ra_1/μ is sufficiently large.

5. Summary

We developed two Gauge–Uzawa schemes, one in conserved form and the other in convective form, for the natural convection problem with variable density, and proved that their first-order versions are unconditionally stable. We believe that the convergence of these schemes can be established with suitable assumptions by following similar procedures in [10]. However, how to prove the stability for their second-order versions is still an open problem.

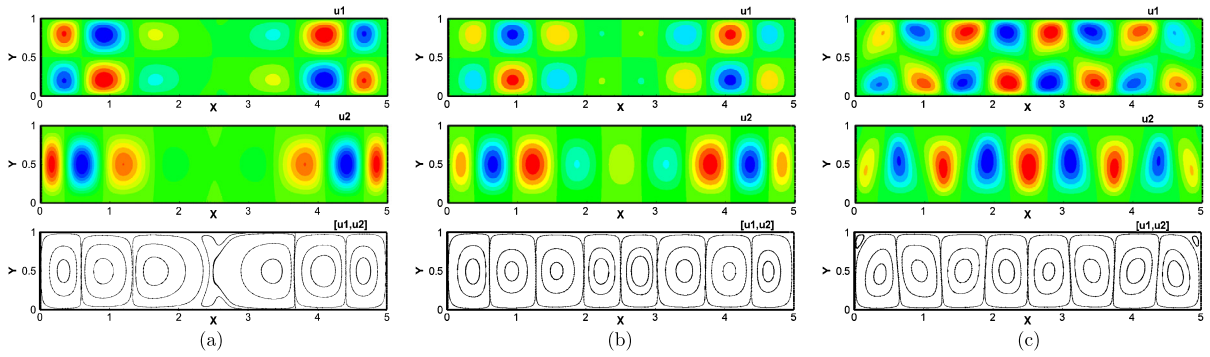

Fig. 9. Velocity of Bénard convection with variable density at $\nu = 1$, $Pr = 1$, $Ra_1 = 10^5$, $\kappa = 1$, $\tau = 10^{-4}$, $h = 1/120$ at different times: (a) $t = 0.02$, (b) $t = 0.05$, (c) $t = 0.08$.

These schemes lead to decoupled elliptic systems for the velocity, the gauge variable and the temperature, respectively. Hence, they are very efficient and easy to implement. We have also presented several numerical tests to validate our analysis and demonstrate the effectiveness of the proposed schemes.

Acknowledgements

The author J. Wu thanks for the financial support from China Scholorship Council. The authors would like to thank the editor and referees for their valuable comments and suggestions which helped us to improve the results of this paper.

References

[1] G. Batchelor, An Introduction to Fluid Dynamics, vol. 1, Cambridge University Press, 1967, pp. 4–252.
[2] J. Boland, W. Layton, An analysis of the finite element method for natural convection problems, Numer. Methods Partial Differ. Equ. 6 (2) (1990) 115–126.
[3] F. Busse, Transition to turbulence in Rayleigh–Bénard convection, in: Hydrodynamic Instabilities and the Transition to Turbulence, Springer, 1981, pp. 97–137.
[4] A. Chorin, J. Marsden, A Mathematical Introduction to Fluid Mechanics, vol. 3, Springer, 1990, pp. 1–45.
[5] G. De Vahl Davis, Natural convection of air in a square cavity: a bench mark numerical solution, Int. J. Numer. Methods Fluids 3 (3) (1983) 249–264.
[6] J. Domaradzki, R. Metcalfe, Direct numerical simulations of the effects of shear on turbulent Rayleigh–Bénard convection, J. Fluid Mech. 193 (1988) 499–531.
[7] W. E, J. Liu, Gauge method for viscous incompressible flows, Commun. Math. Sci. 1 (2) (2003) 317–332.
[8] J. Guermond, L. Quartapelle, A projection FEM for variable density incompressible flows, J. Comput. Phys. 165 (1) (2000) 167–188.
[9] J. Guermond, A. Salgado, A splitting method for incompressible flows with variable density based on a pressure Poisson equation, J. Comput. Phys. 228 (8) (2009) 2834–2846.
[10] J. Guermond, A. Salgado, Error analysis of a fractional time-stepping technique for incompressible flows with variable density, SIAM J. Numer. Anal. 49 (3) (2011) 917–944.
[11] P. Huang, J. Zhao, X. Feng, Highly efficient and local projection-based stabilized finite element method for natural convection problem, Int. J. Heat Mass Transf. 83 (2015) 357–365.
[12] Y. Li, L. Mei, J. Ge, F. Shi, A new fractional time-stepping method for variable density incompressible flows, J. Comput. Phys. 242 (2013) 124–137.
[13] R. Nochetto, J. Pyo, The Gauge–Uzawa finite element method. Part I: The Navier–Stokes equations, SIAM J. Numer. Anal. 43 (3) (2005) 1043–1068.
[14] R. Nochetto, J. Pyo, The Gauge–Uzawa finite element method. Part. II: The Boussinesq equations, Math. Models Methods Appl. Sci. 16 (10) (2006) 1599–1626.
[15] J. Pyo, Error estimates for the second order semi-discrete stabilized Gauge–Uzawa method for the Navier–Stokes equations, Int. J. Numer. Anal. Model. 10 (1) (2013) 24–41.
[16] J. Pyo, J. Shen, Gauge–Uzawa methods for incompressible flows with variable density, J. Comput. Phys. 221 (1) (2007) 181–197.
[17] J. Shen, On error estimates of projection methods for Navier–Stokes equations: first-order schemes, SIAM J. Numer. Anal. 29 (1) (1992) 57–77.
[18] H. Su, X. Feng, Y. He, Defect-correction finite element method based on Crank–Nicolson extrapolation scheme for the transient conduction–convection problem with high Reynolds number, Int. Commun. Heat Mass Transf. 81 (2017) 229–249.
[19] H. Su, X. Feng, Y. He, Second order fully discrete defect-correction scheme for nonstationary conduction–convection problem at high Reynolds number, Numer. Methods Partial Differ. Equ. 33 (3) (2017) 681–703.
[20] K. Szewc, J. Pozorski, A. Taniere, Modeling of natural convection with smoothed particle hydrodynamics: non-Boussinesq formulation, Int. J. Heat Mass Transf. 54 (23) (2011) 4807–4816.
[21] J. Wu, X. Feng, F. Liu, Pressure-correction projection FEM for time-dependent natural convection problem, Commun. Comput. Phys. 21 (2017) 1090–1117.
[22] J. Wu, D. Gui, D. Liu, X. Feng, The characteristic variational multiscale method for time dependent conduction–convection problems, Int. Commun. Heat Mass Transf. 68 (2015) 58–68.
[23] J. Wu, P. Huang, X. Feng, A new variational multiscale FEM for the steady-state natural convection problem with bubble stabilization, Numer. Heat Transf., Part A, Appl. 68 (7) (2015) 777–796.
[24] J. Wu, P. Huang, X. Feng, D. Liu, An efficient two-step algorithm for steady-state natural convection problem, Int. J. Heat Mass Transf. 101 (2016) 387–398.
[25] Q. Zhang, T. Jackson, A. Ungan, Numerical modeling of microwave induced natural convection, Int. J. Heat Mass Transf. 43 (12) (2000) 2141–2154.
[26] T. Zhang, X. Feng, J. Yuan, Implicit–explicit schemes of finite element method for the non-stationary thermal convection problems with temperature-dependent coefficients, Int. Commun. Heat Mass Transf. 76 (2016) 325–336.